JJAP Series 4
Proc. of 1990 Intern. MicroProcess Conference pp. 32–38

New Alignment Sensors for Optical Lithography

Nobutaka MAGOME, Kazuya OTA and Kenji NISHI

System Designing Section, Designing Department,
Industrial Supplies & Equipment Division, Nikon Corporation,
6-3, Nishi-Ohi, 1-Chome, Shinagawa-Ku, Tokyo 140

(Received July 17, 1990; accepted for publication September 22, 1990)

Two alignment sensors, which will be used in half-micron and sub-half-micron lithography, have been newly developed and tested. Both were developed to improve overlay accuracy on some particular types of processed layers with which the current alignment system has problems. One has an incoherent illumination and bright field imaging system with the aim being to reduce scaling and random errors on Al layers. The other is an optical heterodyne sensor of which the aims are to reduce random errors on Al layers and increase the signal detecting capability for small step height marks. These sensors proved to be effective on most difficult layers, and they have practical throughput.

KEYWORDS: optical lithography, alignment, laser alignment, coherence, incoherent illumination, optical heterodyne

§1. Introduction

Historically, steppers with dark field laser alignment systems have dominated LSI production.[1] Recently, however, tighter overlay requirements have revealed problems inherent to coherent dark field alignment systems on some Al layers. Rough Al layers cause random alignment errors, and the asymmetry of the alignment marks and photoresist coating produces scaling error. These errors are usually amplified by the interference effect under coherent illumination.[2]

In order to reduce this coherent phenomenon, multiwavelength illumination methods were studied, and proved to improve the alignment accuracy.[3,4] On the other hand, in the system of dark field type with a narrow laser beam, its alignment signal is sometimes so distorted due to the asymmetric structure of the alignment mark so as to produce a scaling error of more than 3 ppm. Thus, one of the new sensors, FIA (field image alignment), is designed to be a bright field system with incoherent illumination to recognize the alignment mark edges correctly in order to reduce random and scaling errors.

Next, the diffraction grating alignment technique has been studied in X-ray lithography,[5,6] and several of this type have been developed to be adopted on optical step and repeat systems.[7–9] These systems have shown high alignment accuracy and resolution in experiments, and have been used in the LSI production field.[10] We have also studied and developed one of this type, and applied it to a stepper, named LIA (laser interferometric alignment).[11] The developed system, which is based on optical heterodyne interferometry, not only has very high positional resolution and recognition abilities for very rough surfaces, but also high baseline offset stability. This LIA is expected to be effective in aligning planarized layers.

§2. Laser Beam Scanning Alignment System and Alignment Errors on Al Layers

Laser alignment systems, especially the dark field laser scanning type (diffracted or scattered light detection type), have high sensitivity and recognition ability due to the coherency of laser beam.

Overlay accuracy, however, for wafers sputtered with Al are usually worse than for other layers. As contact holes become deeper, higher sputter temperature is required and new metallization techniques such as the use of W or a Ti-CVD (chemical vapor deposition) layer are developed. These types of processing tend to encourage the formation of a rough surface and asymmetrical alignment marks. Figure 1 shows a schematic diagram of a typical alignment mark construction of an Al layer. In this example, a symmetrical concave alignment mark is formed by dry etching, the profile is deformed by the shadowing effect during Al sputtering, and Al grains grow by recrystallization.

In order to reduce random errors caused by the rough metal surface, a multimark averaging method and EGA[12] (enhanced global alignment) were developed. In the multimark method, a plural number of alignment marks is arranged in parallel in a small area of the chip, and each position is measured and averaged to obtain the alignment position. As the number of marks increased, the random deviation of the alignment position decreases by averaging the random effects such as aluminum grains. The EGA method is based on a statistical modeling technique which consists of three steps: measuring, modeling and exposure, as shown in Fig. 2. Firstly, several chips are selected beforehand for measuring. Next, the exposing grid of chip arrangement is calculated to minimize the root mean square errors between designed and measured chip positions. The new coordinates of the chip arrangement are approximated as a linear function of six parameters (means for X and Y, scaling for X and Y, rotation and orthogonality of coordinates). Since most of the wafers have little nonlinear deformation, EGA can correctly approximate the exposing grid. The number of sampling shots is selected according to the roughness of the wafer surface, which is usually more than 10 chips for Al wafers. Then, all chips are exposed by following the calculated grid. The effectiveness of this method has been well proven in the LSI production field.

Error caused by asymmetrical alignment marks, on the

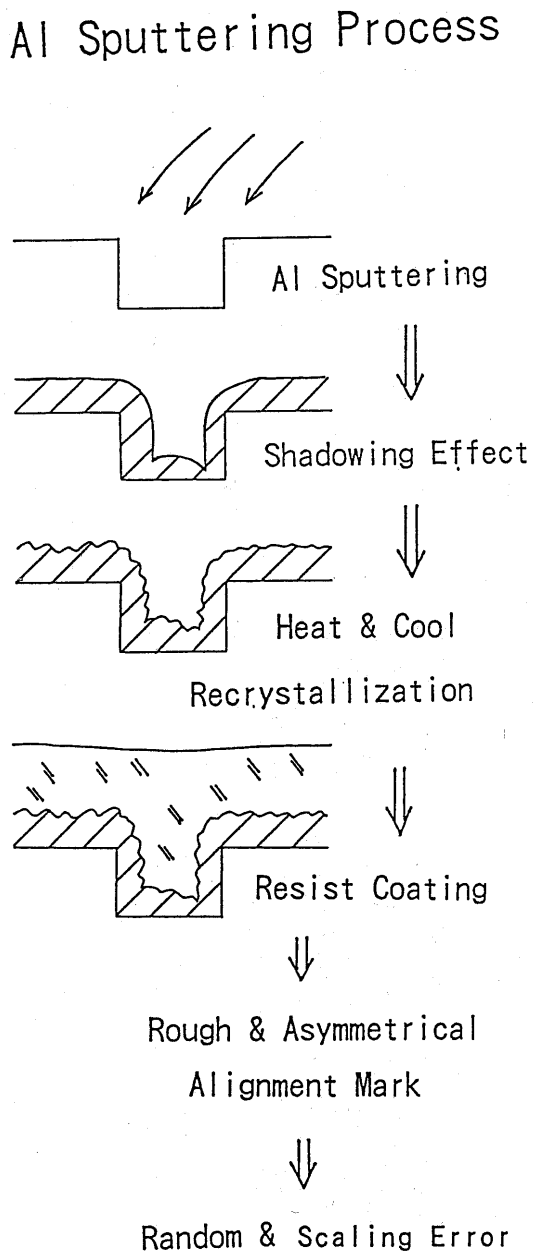

Fig. 1. Al sputtering process and cross sectional shapes of a concave alignment mark. The alignment mark has asymmetrical profile and rough surface due to shadowing effect and thermal process, respectively.

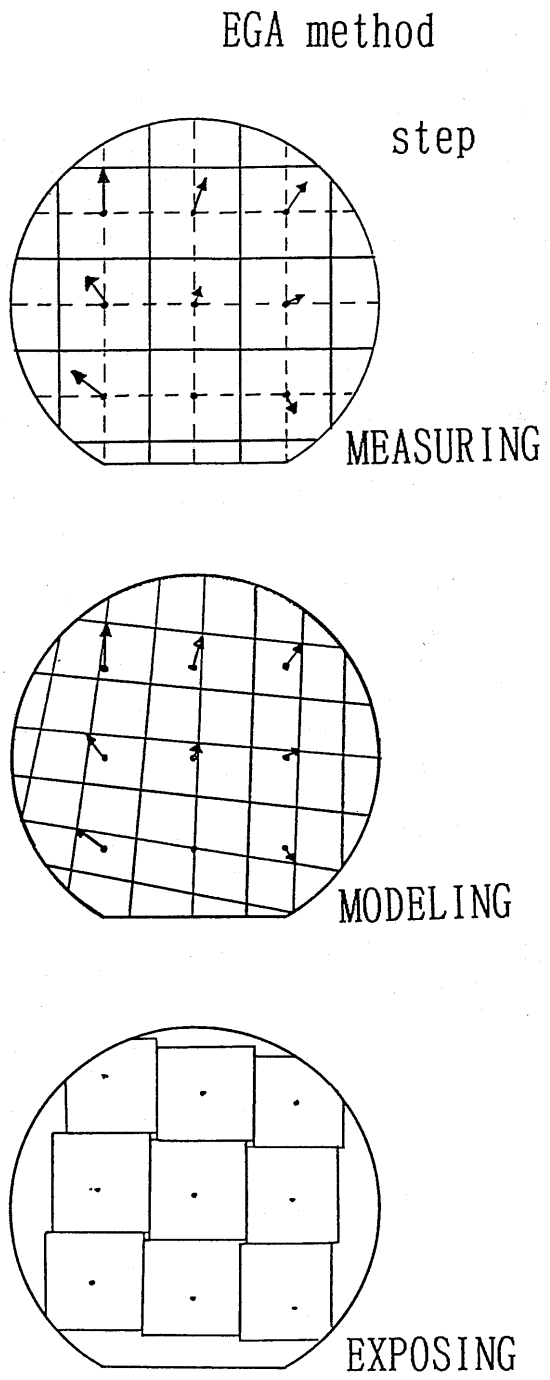

Fig. 2. The EGA alignment sequence is shown. EGA consists of three steps as measuring, modeling and exposing. EGA can reduce random error by averaging plural measured data.

other hand, cannot be corrected using this averaging technique, because the asymmetry of the alignment marks occur systematically rather than randomly. The asymmetrical profile of these marks is a proportional function of radial position with respect to the wafer center; thus, a scaling error is caused. In order to minimize this error, an alignment optimization technique can be adopted. The variables which are optimized are the mark width, the mark duty and the software algorithm.

In most cases, the averaging and optimizing techniques yield good alignment results. There are some layers, however, where a more advanced alignment technique must be used.

§2. FIA

The purpose of FIA is the improvement of alignment accuracy on Al layers by reducing the scaling error. The main features are incoherent illumination and bright field imaging. The use of coherent illumination can cause interference fringes from the multiple reflections off and on the alignment marks. These fringes usually distort the alignment mark image and cause pseudoalignment signals, despite the use of a bright field imaging system. Incoherent illumination light has therefore been adopted.

2.1 *Incoherent illumination*

In the case of a photoresist and substrate system, interference fringes are basically constructed by superimposing two beams: the reflected light from the surface of the photoresist and from the substrate. If the optical path difference of the two light beams is longer than the coherence length of the beams, interference fringes are not observed, referring to Fig. 3.

The following explanation discusses how this incoherent condition is designed. The optical path difference is defined by $2nd$ where n and d denote the refractive index and thickness of the photoresist, respectively, and the coherence length is defined by L^2/dL, where L is the center wavelength and dL is the spectral bandwidth of a given illumination light.

Then an incoherent condition is obtained when

$$2nd > L^2/dL.$$

As a conservative value of photoresist conditions on Al layers, 0.5 μm for d and 1.5 for n are assumed and L is selected as 600 nm. Then the dL necessary to satisfy the incoherent condition must be greater than 240 nm.

The experimental results of coherent effects are shown in Fig. 4. These photographs are microscopic images of the same alignment marks of 0.5 μ height on an Al wafer covered with photoresist of 1 μm thickness under three different illumination conditions. The three graphs on the right show the alignment signal corresponding to each picture.

Under a HeNe laser illumination, high contrast fringes are observed around alignment marks causing inclination of the alignment signal and pseudoalignment signals. These effects greatly affect the alignment accuracy. Using a 40 nm band width, the fringes are hardly visible, but the beginning of the alignment signal is still distorted by the interference effect. Finally, when the width is greater than 200 nm, the fringes disappear, and a clear signal is obtained. This corresponds with the theory presented earlier and justifies the use of a bandwidth greater than 250 nm for the FIA system. The photoresist is insensitive to light of this range.

The FIA optics and electronic system is shown in Fig. 5. Because of the chromatic aberration of the projection lens for the broad band illumination, the alignment scope is mounted beside the projection lens. Despite this, the measured baseline stability was observed to be less than 0.05 μm over 3 hours in Fig. 6.

2.2 *Alignment results by FIA*

As an example of a current dark field alignment system, the LSA (laser step alignment)[1] sensor is used in this experiment. The LSA consists of a stationary laser

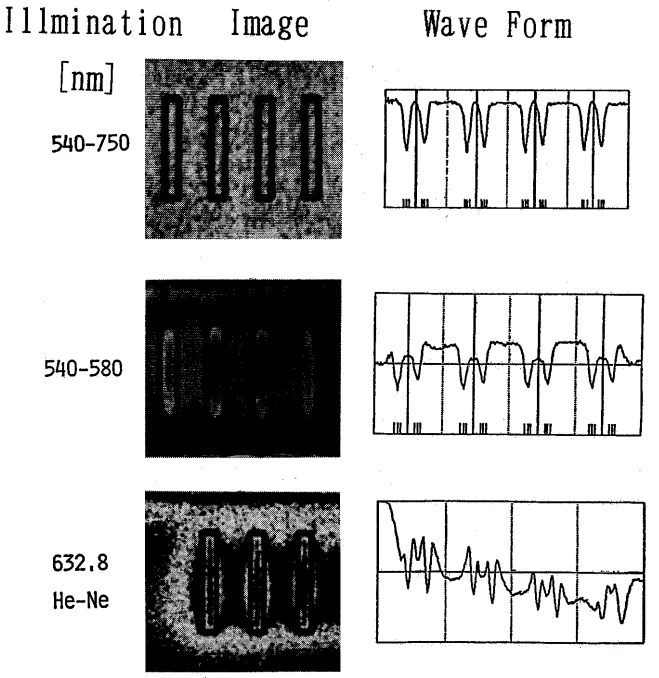

Fig. 4. The experimental results of coherence effects. These photographs are FIA microscopic images of the same alignment marks of 0.5 μm step height with 1 μm thickness photoresist, under three different illumination conditions. The three graphs show the alignment wave corresponding to each picture.

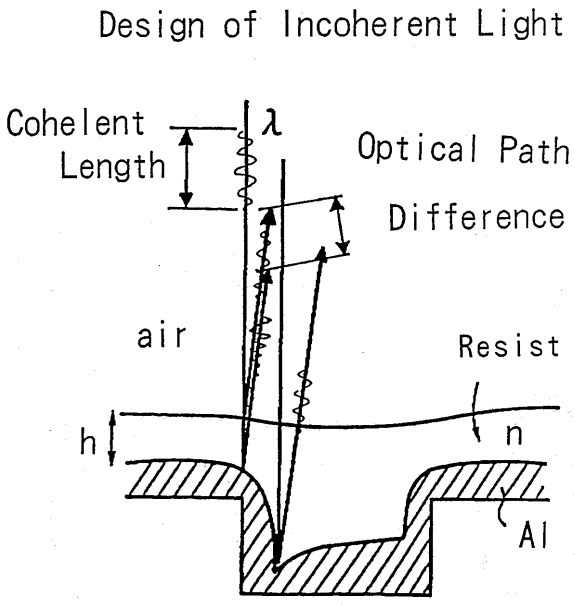

Fig. 3. Incoherent condition of a photoresist and Al layer system is shown. When the optical path difference of the primary reflected two beams is longer than the coherent length of the beams, incoherent condition is satisfied.

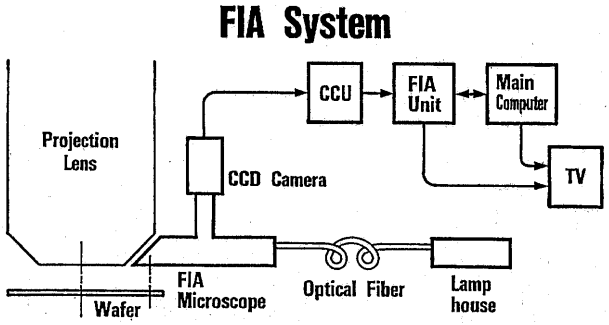

Fig. 5. The schematic diagram of FIA system is shown. The FIA scope is mounted beside the projection lens. The image of wafer alignment mark is processed by FIA unit.

sheet beam passing through the projection lens to the wafer surface, as shown in Fig. 7. The beam undergoes diffraction by the alignment mark when wafer passes beneath it. A detector monitors specific diffraction orders of the light returning from the wafer through the lens. The signal is sampled with wafer position pulses of 0.02 μm interval. The mark position is then calculated from this signal in a microprocessor.

Experimental results of the LSA and FIA overlays are shown in Figs. 8 and 9, respectively. These figures show the overlay accuracy (3 sigma) and residual scaling errors for about 30 Al wafers with varying surface conditions. In Fig. 9, the wafers aligned using FIA show a residual scaling error of less than 1.5 ppm. All wafers were aligned using the 10-point EGA sequence (10 chips are selected for EGA measurement), so residual random errors are small in which the factor of 3 sigma is almost the scaling error because 1 ppm of scaling corresponds to about 0.1 μm of 3 sigma in a 5-inch wafer. Overlay results were measured using either verniers or a scanning electron microscope (SEM). All alignment results of LSA and FIA, including the baseline stability data, were obtained on the same stepper, so the wafer stage conditions were the same.

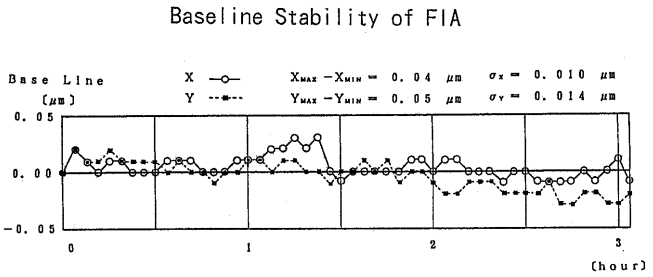

Fig. 6. Baseline stability of FIA is measured. The range is less than 0.05 μm over 3 hours.

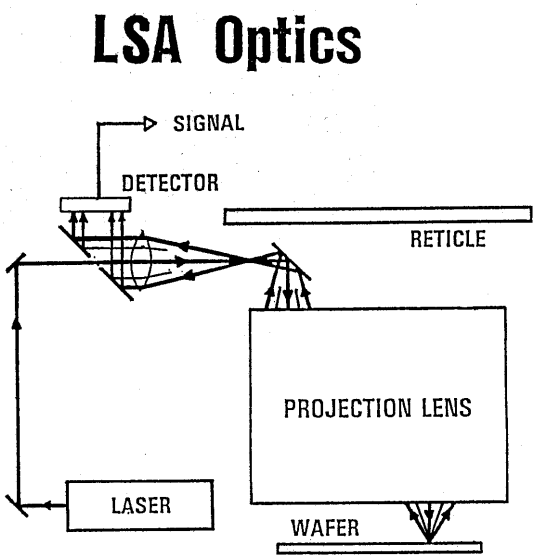

Fig. 7. The schematic diagram of LSA, which is one of TTL sensors, is shown. The laser beam spot is focused on a wafer alignment mark, and the only diffracted light is detected.

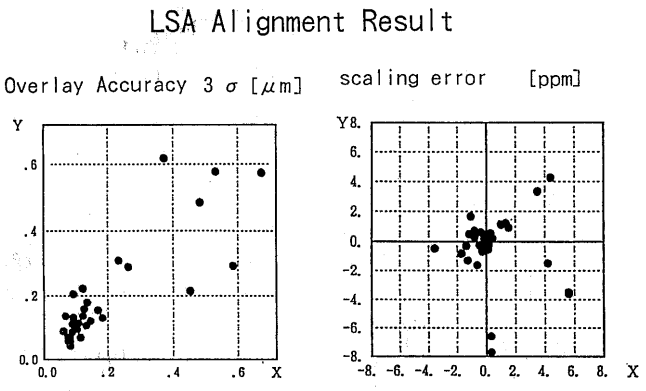

Fig. 8. LSA Alignment Results; the left graph shows the overlay accuracy (3-sigma) in μm, while the right shows the residual scaling factors of x and y directions in ppm. These data include the results measured by nonoptimized parameter settings.

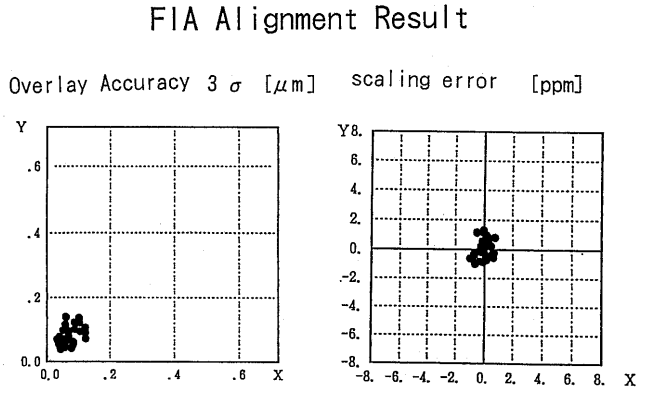

Fig. 9. FIA Alignment Results; the graphs show the same kinds of data as in Fig. 8. The same wafers were used for LSA and FIA experiments. The residual scaling errors are less than 1.5 ppm.

§3. LIA

The LIA is based on optical heterodyne interferometry and has high sensitivity, stability and resolving power. These features result from an optical averaging method over a large illumination area, a high S/N ratio inherent to the phase detection of AC signals of the heterodyne technique, and the use of reference grating to cancel laser fluctuation effects.

The LIA optical system is shown in Fig. 10. Diffraction gratings of 8 μm pitch are used for the LIA alignment marks. Two laser beams with opposite incident angles and slightly different frequencies illuminate these gratings. In order to generate laser beams with different frequencies, two AOMs (acousto optical modulator) are used. One of the AOMs is driven by VHF, the frequency of which is F1 Hz, and the other is driven at F2 Hz. The modulated laser beams incident on the wafer alignment grating are diffracted to some orders, shown in Fig. 11. The $+1$st order of the right incident beam and the -1st order of the left incident beam are diffracted in the same direction, and go back through the projection lens to the detector. This signal is always sinusoidal with a fre-

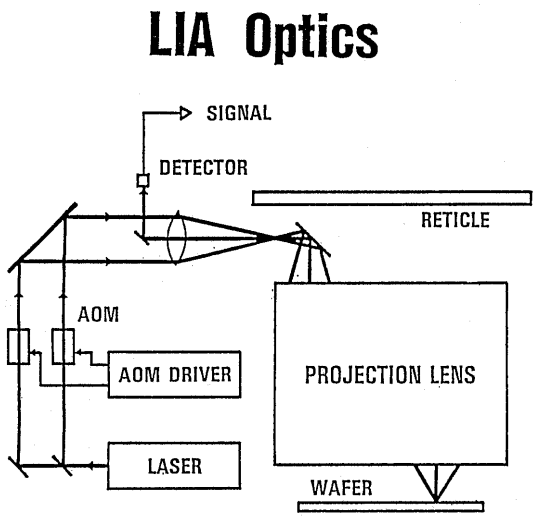

Fig. 10. The schematic diagram of LIA system, that is also one kind of TTL sensors. The frequency modulated beams are made by AOMs, which are driven at the frequency of F1 and F2.

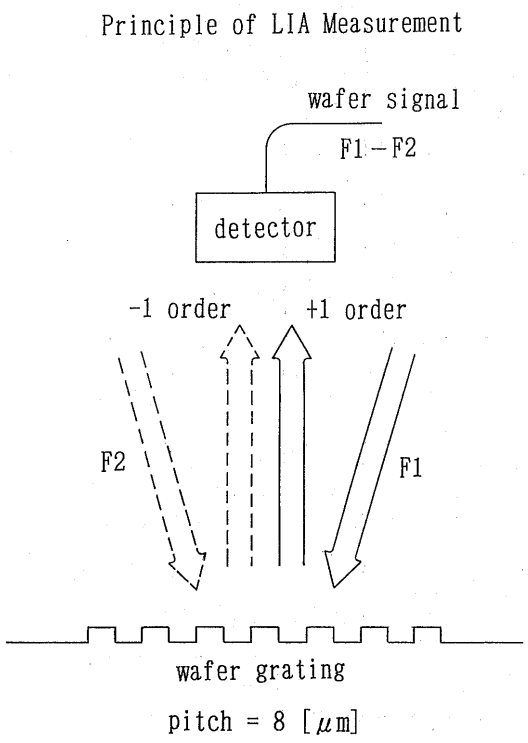

Fig. 11. The principle of LIA measuring method is shown. The diffraction beams of LIA illumination laser light are shown. The right and left incident beams are modulated by frequency F1 and F2, respectively. The 1st order of the right and the −1st order of the left beams are detected. The detected wafer alignment signal is the beat signal of which frequency is F1-F2.

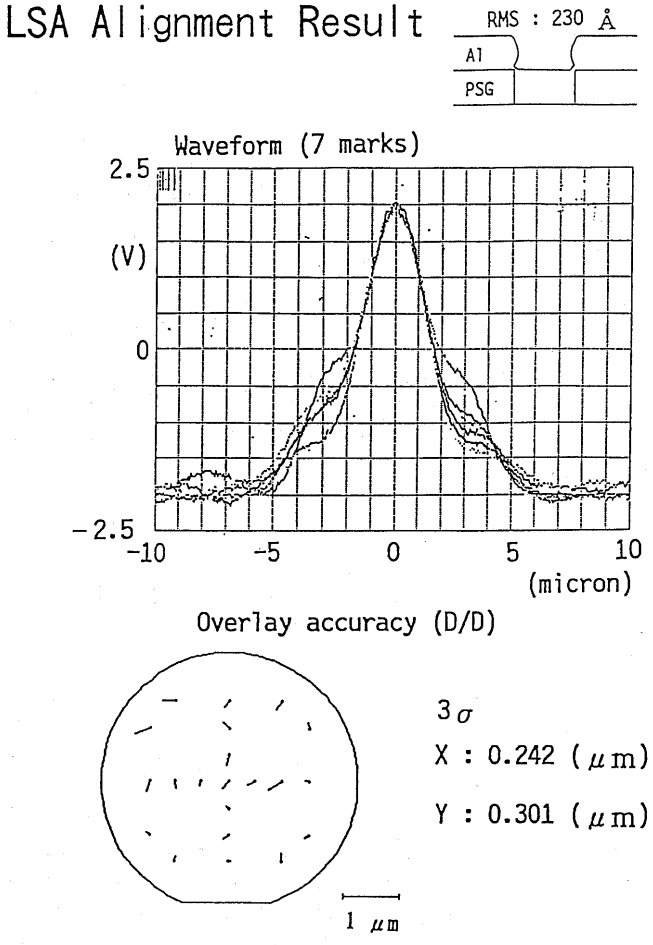

Fig. 12(a). Alignment signals and vector map of LSA result. The 7 alignment signals of one multi-mark are drawn in the same position. Every wave form resemble each other. The roughness of Al surface is 25 nm rms.

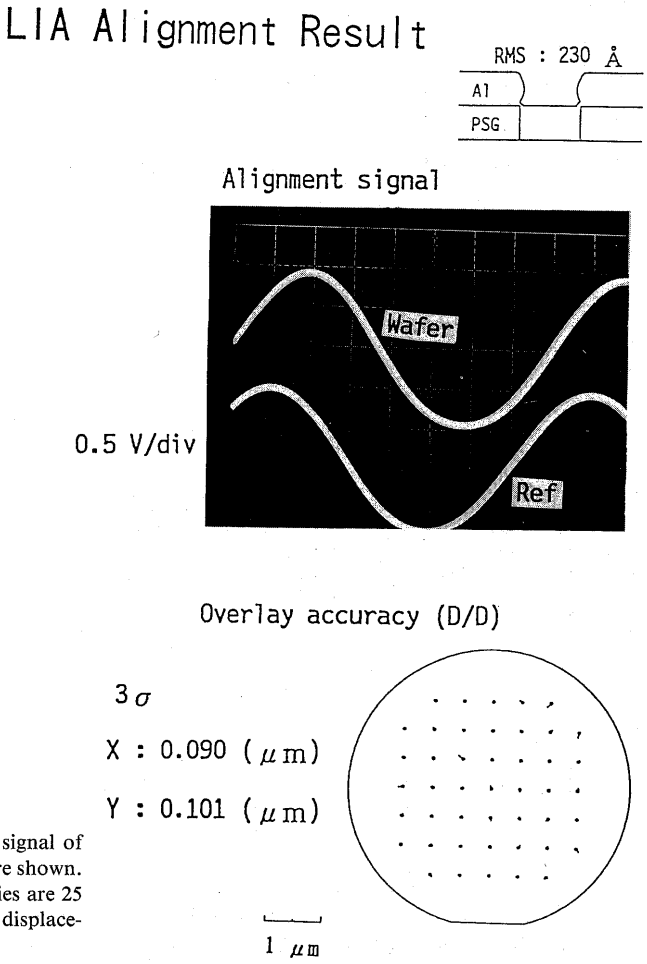

Fig. 12(b). A picture of an alignment signal and reference signal of LIA and alignment results of the same wafer as Fig. 12(a) are shown. The two signals are sinusoidal wave forms whose frequencies are 25 kHz, and the phase difference is proportional to the wafer displacement.

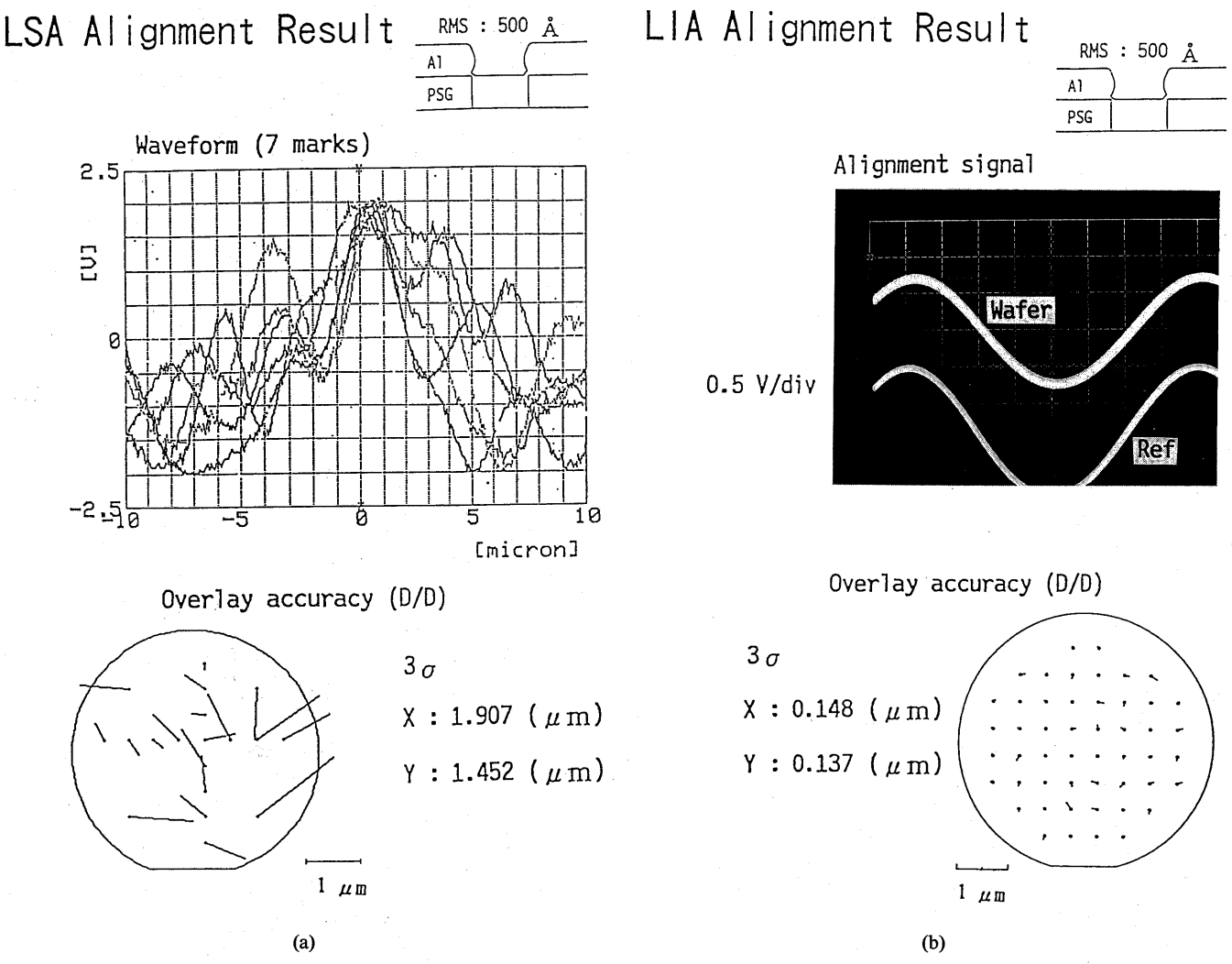

Fig. 13(a),(b). Alignment results of Al wafer with 50 nm rums roughness. The LSA wave forms are degraded remarkably, however, the signal of LIA is stable. The overlay accuracy is obtained less than 1.5 μm (3 sigma) by LIA.

quency equal to the frequency difference (F1-F2 Hz) of the two incident laser beams, even when the roughness of the wafer is considerable. As LIA detects the phase of only 4-μm-pitch spatial frequency from the illumination area, the signal has a high S/N ratio because the distribution of Al grains is so random that the 4 μm spatial frequency component of the Al grains is small.

Wafer position is calculated by measuring the phase angle of the wafer signal. A phase difference of 360 degrees corresponds to 4 μm. The measured phase angle repeats with every 4 μm of wafer displacement. This indicates that the prealignment for this system must be within 2 μm. Also, a phase angle of 0.1 degrees is easily detected and corresponds to approximately 1 nm of diaplacement. Thus, LIA has a high positional resolution, and the actual resolution is limited to about 0.01 μm. This is because the wafer stage positioning control system, which uses a laser interferometer in air, is affected by the air turbulance.

Experimental results on rough Al layers are shown in Figs. 12(a), 12(b) and 13(a), 13(b). Figures 12(a) and 13(a) show LSA results, the upper graphs show LSA waveforms of 7 multimarks (overwritten), and the lower graphs are alignment map details. Figures 12(b) and 13(b) show waveforms of LIA signals and reference signals and LIA alignment results. The wafer in Fig. 13 was very rough (50 nm rms) and had a milky appearance. The LSA waveforms are affected by the roughness of the Al surface. However, the LIA signals (the beat frequency is 25 kHz) are extremely stable and give good alignment accuracy. One of the reasons for the S/N ratio difference is illumination area size. The beam size of LSA is about 2.5 μm × 50 μm, and that of LIA is 50 μm × 80 μm, so the LSA signal can easily pick up Al grains and be very noisy. The LIA can average out these granular surface effects by a large illumination area, and additional electrical noise can be suppressed by a digital analysis using a large number of LIA signal. The alignment mark size of FIA is also as large as that of LIA, but LIA has the advantage of a low step alignment mark because of a monochromatic dark field sensor. Also, the offset is very stable, and the data were measured over 7 hours, with the mean value of x and y measured as les than 0.02 μm, as shown in Fig. 14.

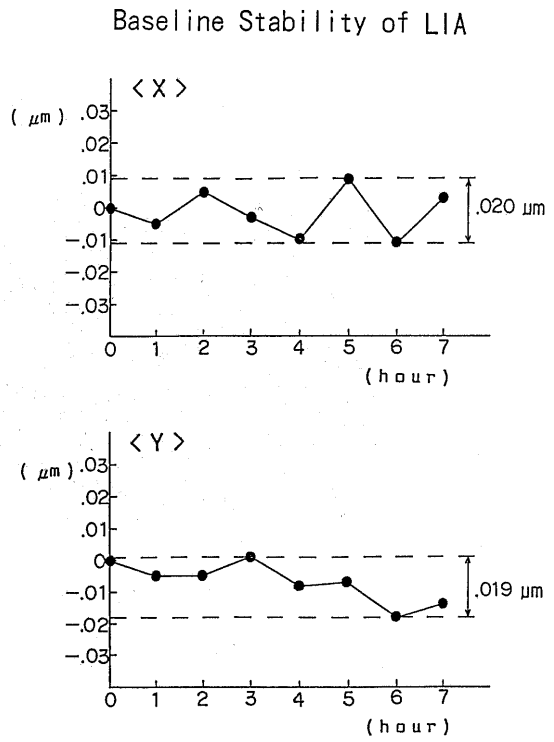

Fig. 14. The baseline stability of LIA are measured, both of X and Y data are less than 0.02 μm over 7 hours.

§4. Conclusions

Two alignment sensors have been developed and tested. Scaling errors were shown to be well corrected using FIA, with residual errors of less than 1.5 ppm. As an image processing method, however, FIA has the disadvantage in that it hardly detects a low contrast image of a very low step height (less than about 50 nm). Its total throughput of a 6-inch wafer using the 10-point EGA method is about 80% that of LSA. On the other hand, LSA and LIA can detect low step marks, but LSA cannot be adopted for very rough wafers. The LIA alignment time of one chip is almost the same as in LSA, but LIA has about 90% of the throughput of LSA when prealignment is necessary. From these features, it is concluded that these sensors combined can align all types of processed wafers if they are properly selected. Thus, the current sensor, LSA, should be used for almost all wafers because of its high throughput except for difficult Al wafers. The FIA should be used for some rough and asymmetrical Al wafers. Also, LIA should be used for rough and very low step height layers such as a planarized wafer. Both of these new sensors, as well as LSA, are expected to be used on excimer, X-ray and SOR lithography systems.

References

1) S. Murakami, T. Matsuura, M. Ogawa and M. Uehara: *Proc. of SPIE 538 Optical Microlithography* **4** (1985).
2) N. Magome and N. Shiraishi: *Proc. of SPIE 1088 Optical/Laser Microlithography* **2** (1989).
3) S. Kuniyoshi, T. Terasawa, T. Kurosaki and T. Kimura: J. Vac. Sci. Technol. **B5(2)** (1987) 555.
4) S. Sugiyama, T. Tawa, Y. Oshida, T. Kurosaki and F. Mizuno: *Proc. of SPIE 922 Optical/Laser Microlithography* (1988) 318.
5) D. C. Flanders, H. I. Smith and S. Austine: Appl. Phys. Lett. **31** (1977) 426.
6) A. Une, M. Inoshiro, M. Suzuki and Y. Torii: *Proc. of JJAP 47th Conf. 28a-ZF-6, -10* (1986 Autumn) [in Japanese].
7) G. Bouwhuis and S. Wittekoek: *IEEE Trans. on ED* **26** (1979) 723.
8) N. Nomura, T. Matsumura, T. Yonezawa and K. Kugimiya: *JJAP* **24** (1985) 1555.
9) N. Nomura, K. Yamashita, Y. Yamada, M. Suzuki and T. Takemoto: *JJAP* **26** (1987) 959.
10) M. A. v. d. Brink, H. F. D. Linders and S. Wittekoek: *Proc. of SPIE* **633** (1986) 60.
11) N. Magome, H. Mizutani, K. Ota and K. Komatsu: *Proc. of JJAP 50th Conf. 29a-L-2* (1989 Autumn) [in Japanese].
12) S. Slonaker, S. McNamara, K. Konno, R. Miller, S. Murakami, N. Magome, T. Umatate and H. Tateno: *Proc. of SPIE 992 Optical/Laser Microlithography* (1988).